

One multi-model flood forecasting system for the Po Delta region developed

Final version June 2023
Deliverable number 5.3.1.

Project Acronym STREAM
Project ID Number 10249186
Project Title Strategic Development of Flood Management
Priority Axis 2 – Safety and Resilience
Specific objective 2.2 – Increase the safety of the Programme area from natural and man-made disaster

Work Package 5
Work Package Title Pilot projects
Activity Number 5.3
Activity Title Po Delta pilot site
Partner in Charge LP
Partners involved PP4, PP6, PP7
Status Final
Distribution Public

TABLE OF CONTENTS

Introduction	4
CHAPTER 1 - FOREWORD	5
CHAPTER 2 - THE MULTI MODEL FLOOD FORECASTING SYSTEM FOR THE PO DELTA REGION	6
2.1 STUDY AREA AND MODEL IMPLEMENTATION	6
2.2 MODEL CALIBRATION.....	8
2.3 MODEL VALIDATION	23
2.4 OPERATIONAL IMPLEMENTATION AND PRODUCTS.....	30
CONCLUSIONS	35
REFERENCES	37

Introduction

During the STREAM project, a new implementation of the hydrodynamics model SHYFEM was conducted. The new set-up comprehends a very high-resolution domain of the Po Delta (reaching all the way upstream to the Pontelagoscuro station in the Po River) and the Emilia-Romagna region. The model implementation followed previous studies which confirmed the aptitude of SHYFEM to reproduce the meteo-marine conditions in the area also associated with the river boundary conditions. A calibration-validation approach was followed with which an optimized set of parameter values decided on. After, the model was operationally implemented providing +72h of forecasts and adding value in terms of high-resolution process solving that currently implemented models do not provide.

CHAPTER 1 - FOREWORD

The multi model flood forecasting system for the Po Delta region has been conceptualized for several reasons, including the limitations of currently operational finite difference models on reproducing complex bathymetries and the misrepresentation that is normally associated by dividing the Po Delta branches' discharge and how they get into the surrounding Adriatic Sea. Hence, the development and implementation of a finite element model such as the System of Hydrodynamics Modules (ShyFem) allowing for an accurate representation of the Po Delta system including its branches and associated lagoons is definitely a step forward in what refers to very high-resolution coastal modelling.

In an operational context, appropriately depicting the effects of high sea levels, whether the combination of astronomical and meteorological components or each of them alone, associated with river discharge and high incoming waves is still a challenge due to model capacity and domain representation limitations. However, two of the aforementioned challenges (river discharge and sea level) can be overcome with the domain implemented during the STREAM project as shown in Figure 1. By combining the high-resolution atmospheric forcing from COSMO-2I and COSMO-5M, river discharges and oceanographic boundaries from an Adriatic, ROMS-based model it is possible for the first time to have a forecasting implementation that allows for the representation of the Po Delta and associated systems. This multi-model system implementation is a first of its kind and covers not only the Po Delta system but also the Emilia-Romagna Regional coastline.

Storm surge forecasting can be done through the implementation of hydrodynamic models, with examples of operational applications for the coasts of the United Kingdom and the Netherlands. The application of appropriately set, calibrated, and validated hydrodynamic models assumes a key role not only on forecasting and scenario projections, but also in the investigation of past events, which provide fundamental information to better manage future emergencies. In the scope of the project, the hydrodynamics model chosen is the System of Hydrodynamic Finite Element Modules (SHYFEM) (Umgiesser et al., 2004) which has been receiving increasing attention from the scientific community. As a finite element model, SHYFEM allows its application on unstructured triangular grids that provide an advantage when the study site presents a complex bathymetric setting (e.g. shallow waters of coastal areas and shelf seas). In this way, it is possible to vary the triangle sizes depending on the necessity of higher resolutions on specific parts of the modeled domain. SHYFEM's flexibility enables its usage on a variety of environments and for different purposes (e.g. Bellafiore and Umgiesser, 2010; Chikita et al., 2015; Cucco and Umgiesser, 2006; De Pascalis et al., 2012).

In the following chapter and subchapters, the study area is briefly described and the flood forecasting system explained in depth with specific technical characteristics. Subsequently, the results of the model calibration and validation are shown followed by some of the operational results provided on a daily basis.

CHAPTER 2 - THE MULTI MODEL FLOOD FORECASTING SYSTEM FOR THE PO DELTA REGION

2.1 STUDY AREA AND MODEL IMPLEMENTATION

The Shyfer model domain covering the Po Delta + Emilia-Romagna (shyFER hereinafter) consists of 45400 nodes and 81879 elements with a maximum depth reaching 55m offshore (27 z levels in total). Its bathymetry has been generated by combining in situ measurements (single and multibeam data for the coastal areas and Po river branches) with the EMODNET2020 gridded values ($\approx 115\text{m}$ for the offshore locations where measurements were not available).

In what refers to the atmospheric forcing of the system, two different numerical weather prediction (NWP) models that follow the Consortium for Small-Scale Modeling (COSMO) implementations in Italy (Steppeler et al., 2003) were used. COSMO provides two domains: one covering the whole Mediterranean with a horizontal resolution of 5km (with forecasts up to +72h - COSMO-5M) and one covering only the Italian territory with a higher resolution of 2.2km (with forecasts up to +48h - COSMO-2I). The COSMO modeled outputs are used as atmospheric forcing in the calibration and validation simulations as well as in the forecasting system operationally implemented. In what refers to the calibration and validation simulations, the analyses outputs of COSMO-2I were used whenever available while in the days in which those outputs were not at one's disposal, the analyses of COSMO-5M were then applied. In the operational shyFER forecasting implementation, the atmospheric analyses of COSMO-2I are used on a daily basis from hour -24h to hour +48h and COSMO-5M is used to cover the remaining period up to +72h.

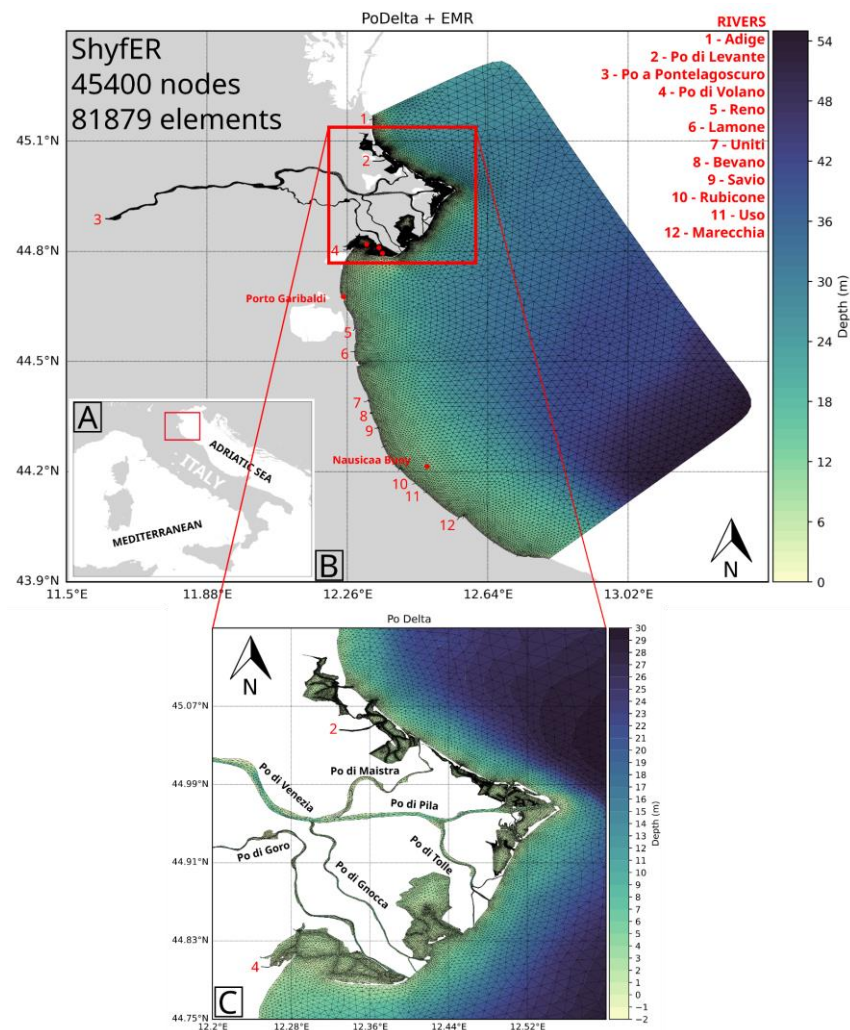


Figure 1: A) Context map showing the location of the Po Delta + Emilia-Romagna domain within the Mediterranean and Adriatic basins. B) The numerical domain (colorbar presenting the bathymetry) within the Adriatic Sea showing the rivers that are used as hydrologic boundaries (in red with their numbers and names on the top right corner of the image) and the locations of the Nausicaa buoy and the Porto Garibaldi tide gauge (stations that were used in the calibration and validation of the model). C) The area zoomed in showing specifically the Po Delta area with its branches and the lagoon systems associated with it.

Oceanographic boundaries were collected from an Adriatic (AdriaC) implementation of the Regional Ocean Modeling System (ROMS) online coupled with the Simulating WAVes Nearshore (SWAN) wave model known as COAWST (Warner et al., 2010). AdriaC is run in a curvilinear orthogonal grid (on a Lambert Conformal Conic cartographic projection) regularly spaced in one kilometer, with 30 vertical terrain-following (sigma) levels. At the open oceanographic boundaries, the outputs of AdriaC in terms of salinity, temperature and total water level were propagated in the shyfer

domain. For the cal-val simulations, AdriaC analyses were used whenever available while in the days they were missing, previous days' forecasts were then used in order to have the best possible open oceanographic boundaries. In the operational forecasting system, as AdriaC covers the whole period (from -24h to +72h) its boundaries are used alone, contrary to what occurs with the atmospheric forcing (in which two different forcing models are used due to temporal coverage inconsistencies).

Additionally, the system also comprehends the most important rivers in the region for which observed values for the Po at Pontelagoscuro are used in terms of temperature and discharge. For the other regional rivers, climatological values have been used. In addition to that, three water pumps (Romanina, Bonello and Giralda) that are manually opened and closed depending on the amount of water in the system were also used for the Sacca di Goro. For them, climatological values are used as it is not possible to define a single criterion for when they are open and the real-time amount of freshwater coming into the system. The integration of the Po forecasted discharge from the hydrologic model implemented for the region is still underway. An approach to be followed has already been agreed upon with the hydrology department of Arpae in what refers to model results exchange and how to couple that with the hydrodynamics of shyFER.

2.2 MODEL CALIBRATION

Several calibration simulations were conducted and a brief explanation of the tested conditions is provided below. Due to the high computational burden for running such a detailed numerical domain and taking into consideration the temporal availability of the oceanographic boundary conditions, the year 2021 was selected and divided in two parts: the first half from 01-01-2021 until 30-06-2021 and a second period from 01-07-2021 until 31-12-2021. The first aforementioned period was used for calibration in which the model parameters and setting were tuned until the best results were obtained. This was done by analyzing them relative to pre-established benchmarks (measuring stations along the coast and inside Goro Lagoon - as shown in Figure 1). Total water level, salinity and temperature were the variables used in the analyses.

For the calibration and validation simulations, a spin-up period of two months was considered before beginning with the analyses of the results. This reflects roughly the time necessary for the model to become stable and balance off the different forcing and boundary conditions. Initial temperature and salinity values 10°C and 30PSU were chosen, respectively. Both temperature and salinity were distributed horizontally and vertically in the whole domain which then started

propagating the oceanographic and river boundary conditions and forced by the previously explained atmospheric forcing.

Calibration was performed from an initial set of pre-defined variables based on knowledge acquired during previous, similar experiments and considering the environmental characteristics of the area. The initial parameter set was then slightly modified for a total of eight simulations covering the calibration period. Below, the results obtained for the best calibration set are shown for each station used in the analyses. It is important to emphasize that the analyses performed here do not consider the first two months of the simulation as they are used as spin-up time for the system to reach a stable condition. After the best results were obtained from the set of calibration simulations, the second period was then performed using the best parameter set in what here is referred to as the validation simulation. Validation results are presented in the next section.

The first multi-parameter station for which the model results were confronted was the Gorino station inside Sacca di Goro (Figure 1C). Out of the eight calibration simulations performed, the best results obtained for salinity at the Gorino station refer to the simulation georg51 which reached a Pearson correlation value of 0.42, with a Mean Absolute Error (MAE) of 3.66PSU and a Root-Mean Square Error (RMSE) of 4.60PSU (Table 1). The time series, scatterplot, and the probability density function (PDF) associated with the simulation and the observed values are shown in Figure 2.

Table 1: statistics for salinity at the Gorino measuring station for each of the calibration simulations (SIM) performed. The sampling size is shown below the name of the variable being analyzed. In bold are highlighted the values of the best performance for that specific variable for that specific station.

Gorino	SALINITY (n =2728)							
SIM	georg51	georg52	LargePond	zLBC	zLBC2	SmithBanke	georg50_arpae	Chezy
Pearson	0.42	0.41	0.42	0.40	0.40	0.41	0.41	0.40
MAE	3.66	4.36	3.98	4.31	3.98	4.01	4.38	4.47
RMSE	4.60	5.40	4.95	5.30	4.92	5.01	5.43	5.52

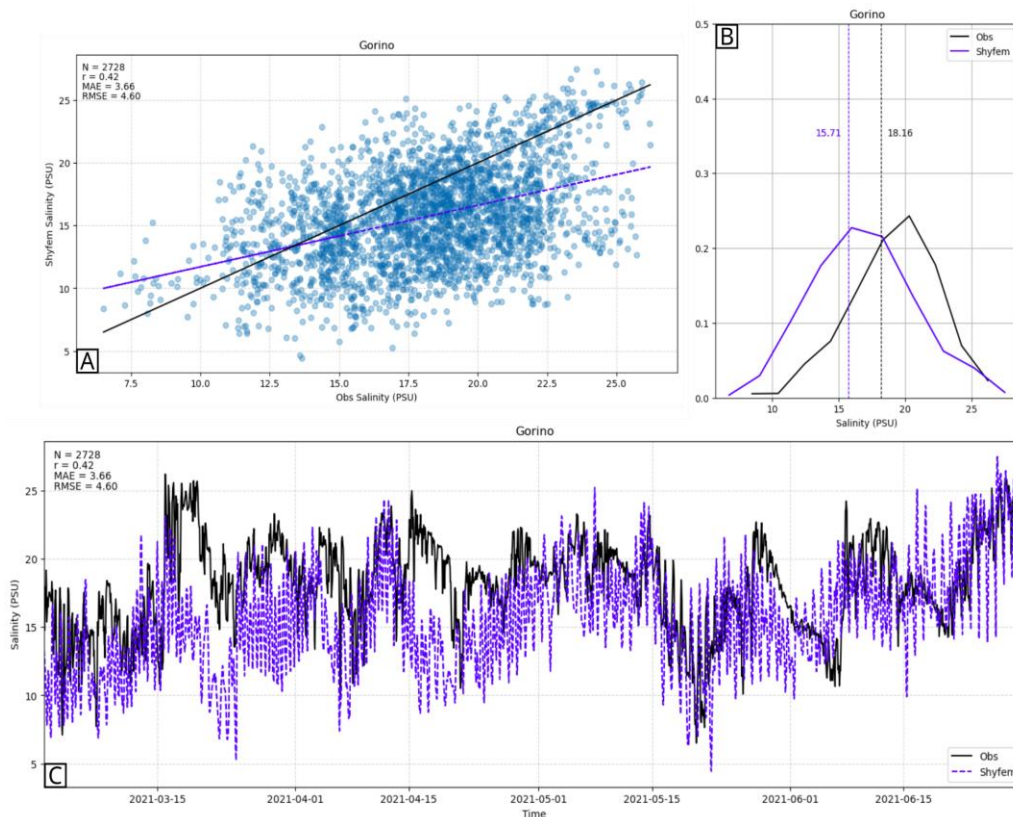


Figure 2: all subplots refer to salinity measurements at the Gorino station and the Shyferm modeled results at the closest possible location. A) scatter plot for measured and simulated salinity where the black line refers to a reference, perfect fit while the regression line in blue relates the observed data with the modeled results. B) probability distribution function for the observed data (black) and the model results (blue). C) time series of the observed data (black solid line) plotted together with the model results (blue dashed line).

A second station called Mitili (also inside Sacca di Goro - Figure 1C) was used for the temperature checking, with the best results referring to the simulation SmithBanke which reached a Pearson correlation coefficient of 0.99, with an MAE of 0.99°C and an RMSE of 1.26°C (Table 2). The time series, scatterplot, and the PDF associated with the simulation georg51 and the observed values are shown in Figure 3.

Table 2: statistics for temperature at the Mitili measuring station for each of the calibration simulations (SIM) performed. The sampling size is shown below the name of the variable being analyzed. In bold are highlighted the values of the best performance for that specific variable for that specific station.

Mitili	TEMPERATURE (n = 2787)							
	georg51	georg52	LargePond	zLBC	zLBC2	SmithBanke	georg50_arpae	Chezy
Pearson	0.99	0.99	0.99	0.99	0.99	0.99	0.99	0.99
MAE	1.03	1.03	1.02	1.06	1.06	0.99	1.03	1.00
RMSE	1.30	1.30	1.29	1.34	1.34	1.26	1.30	1.27

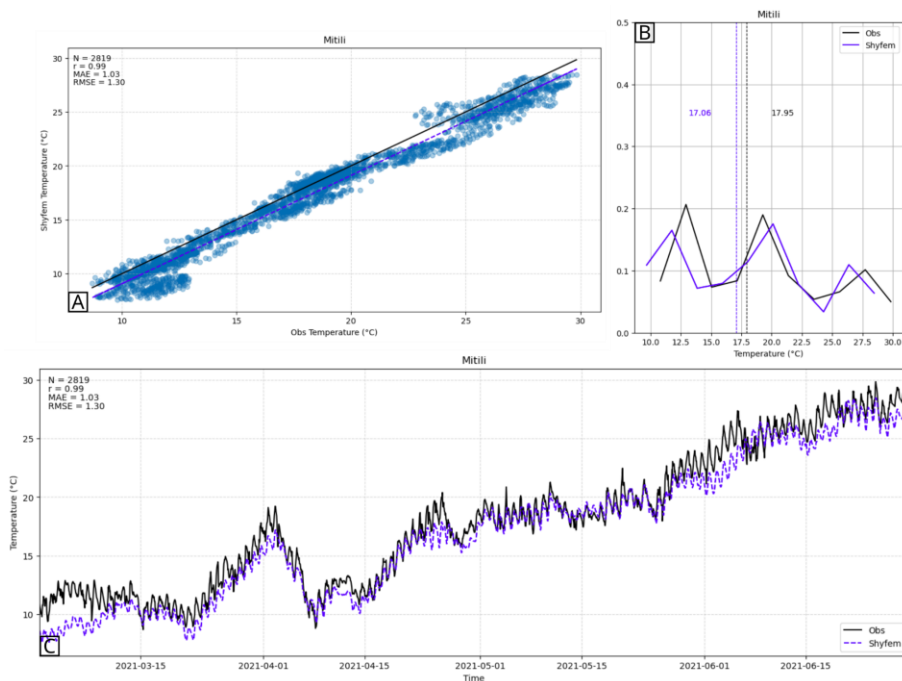


Figure 3: all subplots refer to temperature measurements at the Mitili station and the Shyftm modeled results at the closest possible location. A) scatter plot for measured and simulated temperature where the black line refers to a reference, perfect fit while the regression line in blue relates the observed data with the modeled results. B) probability distribution function for the observed data (black) and the model results (blue). C) time series of the observed data (black solid line) plotted together with the model results (blue dashed line).

A wave buoy (Nausicaa - Figure 1B) located 8km off the coast of Cesenatico was analyzed, with the best temperature representation being difficult to individuate as several simulations had similar statistical values. A Pearson correlation coefficient of 0.99 was observed in all the simulations, with an MAE of 0.84°C and an RMSE of 0.97°C observed in six out of the eight simulations (Table 3). The time series, scatterplot, and the PDF associated with the simulation georg51 and the observed values are shown in Figure 4.

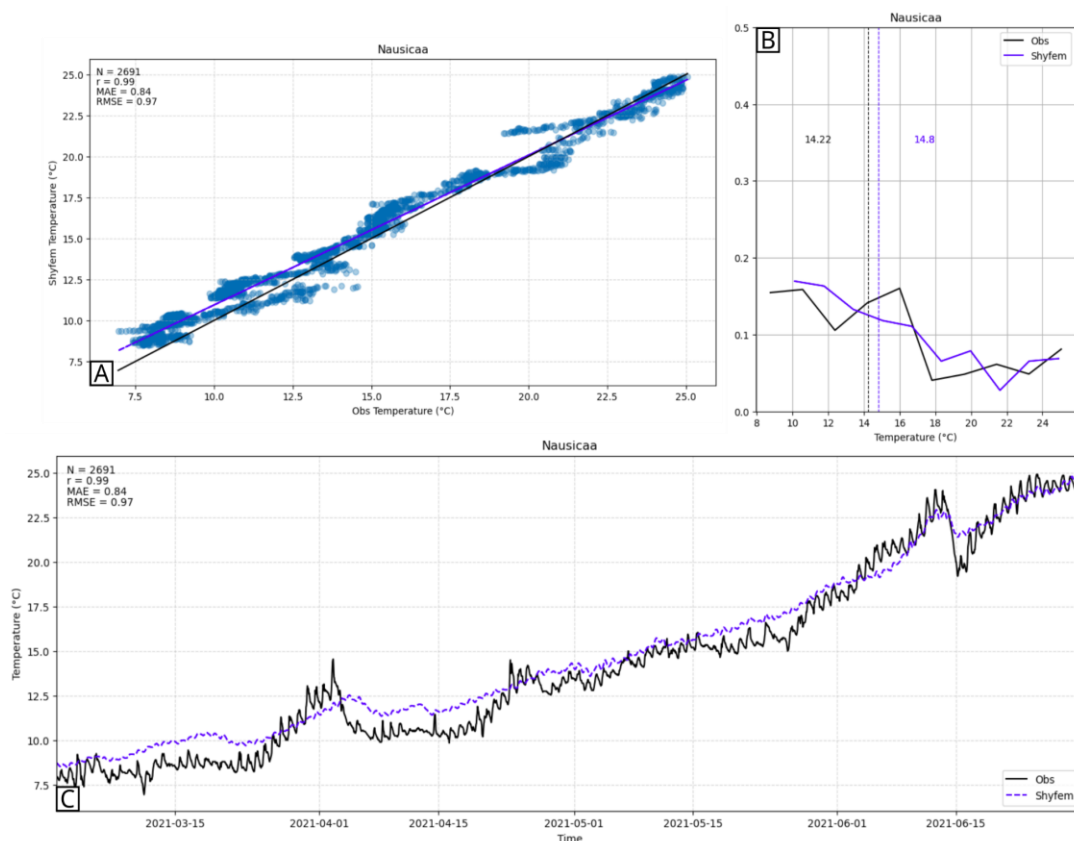


Figure 4: all subplots refer to temperature measurements at the Nausicaa buoy and the Shyferm modeled results at the closest possible location. A) scatter plot for measured and simulated temperature where the black line refers to a reference, perfect fit while the regression line in blue relates the observed data with the modeled results. B) probability distribution function for the observed data (black) and the model results (blue). C) time series of the observed data (black solid line) plotted together with the model results (blue dashed line).

Table 3: statistics for temperature at the Nausicaa buoy for each of the calibration simulations (SIM) performed. The sampling size is shown below the name of the variable being analyzed. In bold are highlighted the values of the best performance for that specific variable for that specific station.

Nausicaa	TEMPERATURE (n = 2691)							
SIM	georg51	georg52	LargePond	zLBC	zLBC2	SmithBanke	georg50_arpae	Chezy
Pearson	0.99	0.99	0.99	0.99	0.99	0.99	0.99	0.99
MAE	0.84	0.84	0.84	0.98	0.98	0.84	0.84	0.84
RMSE	0.97	0.97	0.97	1.16	1.16	0.97	0.97	0.97

For the meteo-marine station of Porto Garibaldi that comprehends a tide gauge and a variety of atmospheric and oceanographic sensors, out of the eight calibration simulations performed, the best results obtained for salinity refer to the simulation LargePond which reached a Pearson correlation coefficient of 0.68, with an MAE of 2.42PSU and an RMSE of 3.20PSU (Table 4). However, the simulations zLBC and zLBC2 outperformed the other six in what refers to the Pearson correlation coefficient (0.70). The time series, scatterplot, and the PDF associated with the simulation georg51 and the observed values are shown in Figure 5.

For the total water level, out of the eight calibration simulations performed, the best results obtained at the Porto Garibaldi are impossible to be individualized as all the simulations presented the same statistical scores (Table 5). The time series, scatterplot, and the PDF associated with the simulation georg51 and the observed values are shown in Figure 6.

For temperature, the best results at the Porto Garibaldi station refer to the simulation georg51 which reached a Pearson correlation value of 0.97, with an MAE of 1.26°C and a RMSE of 1.54°C (Table 6). Three simulations (LargePond, zLBC and zLBC2) outperformed georg51 in what refers to the Pearson correlation coefficient, reaching a value of 0.98. The time series, scatterplot, and the PDF associated with the simulation georg51 and the observed values are shown in Figure 7.

Table 4: statistics for salinity at the Porto Garibaldi measuring station for each of the calibration simulations (SIM) performed. The sampling size is shown below the name of the variable being analyzed. In bold are highlighted the values of the best performance for that specific variable for that specific station.

Porto Garibaldi	SALINITY (n =2765)							
SIM	georg51	georg52	LargePond	zLBC	zLBC2	SmithBanke	georg50_arpae	Chezy
Pearson	0.67	0.67	0.68	0.70	0.70	0.63	0.65	0.66
MAE	2.48	2.47	2.42	2.55	2.56	2.52	2.49	2.52
RMSE	3.26	3.23	3.20	3.34	3.35	3.30	3.25	3.31

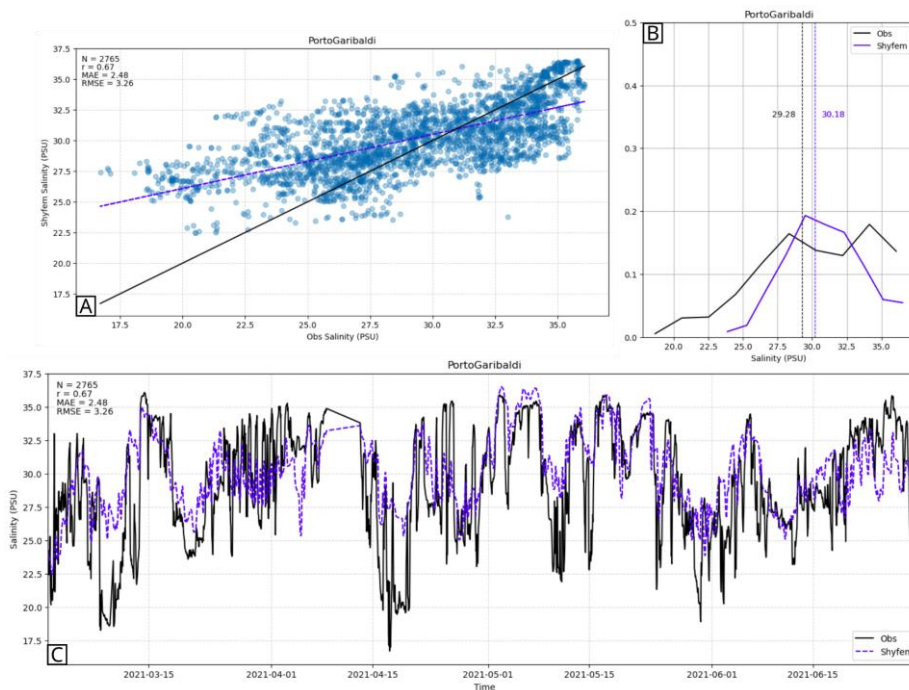


Figure 5: all subplots refer to salinity measurements at the Porto Garibaldi integrated station and the Shyferm modeled results at the closest possible location. A) scatter plot for measured and simulated salinity where the black line refers to a reference, perfect fit while the regression line in blue relates the observed data with the modeled results. B) probability distribution function for the observed data (black) and the model results (blue). C) time series of the observed data (black solid line) plotted together with the model results (blue dashed line).

Table 5: statistics for total water level at the Porto Garibaldi measuring station for each of the calibration simulations (SIM) performed. The sampling size is shown below the name of the variable being analyzed. In bold are highlighted the values of the best performance for that specific variable for that specific station.

Porto Garibaldi	TOTAL WATER LEVEL (n =2903)							
	georg51	georg52	LargePond	zLBC	zLBC2	SmithBanke	georg50_arpae	Chezy
Pearson	0.92	0.92	0.92	0.92	0.92	0.92	0.92	0.92
MAE	0.07	0.07	0.07	0.07	0.07	0.07	0.07	0.07
RMSE	0.09	0.09	0.09	0.09	0.09	0.09	0.09	0.09

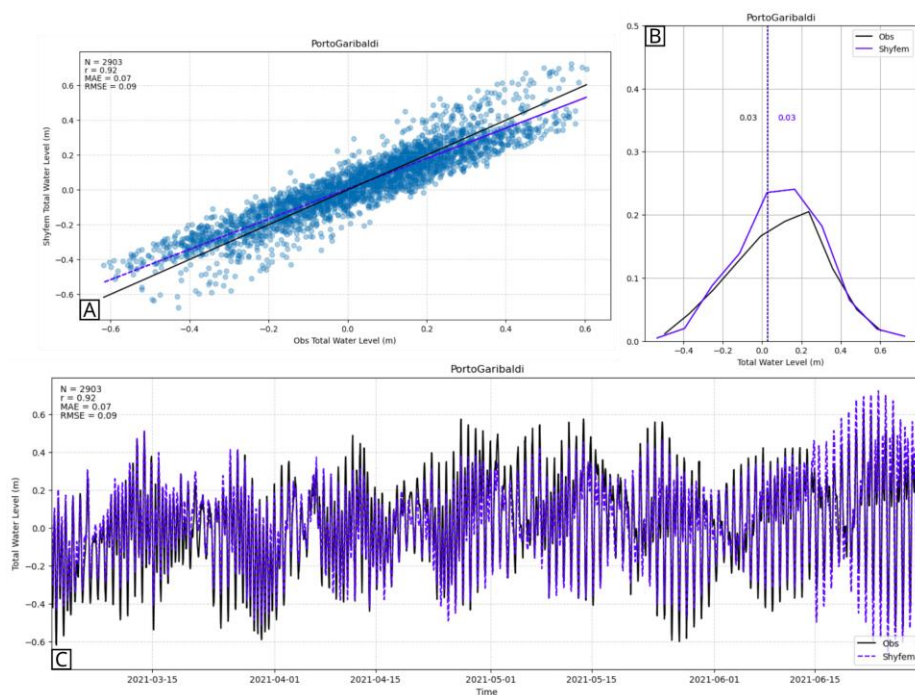


Figure 6: all subplots refer to total water level measurements at the Porto Garibaldi integrated station and the Shyferm modeled results at the closest possible location. A) scatter plot for measured and simulated total water level where the black line refers to a reference, perfect fit while the regression line in blue relates the observed data with the modeled results. B) probability distribution function for the observed data (black) and the model results (blue). C) time series of the observed data (black solid line) plotted together with the model results (blue dashed line).

Table 6: statistics for temperature at the Porto Garibaldi measuring station for each of the calibration simulations (SIM) performed. The sampling size is shown below the name of the variable being analyzed. In bold are highlighted the values of the best performance for that specific variable for that specific station.

Porto Garibaldi	TEMPERATURE (n = 2754)							
SIM	georg51	georg52	LargePond	zLBC	zLBC2	SmithBanke	georg50_arpae	Chezy
Pearson	0.97	0.97	0.98	0.98	0.98	0.97	0.97	0.97
MAE	1.26	1.33	1.31	1.33	1.33	1.28	1.27	1.28
RMSE	1.54	1.62	1.59	1.62	1.62	1.56	1.55	1.55

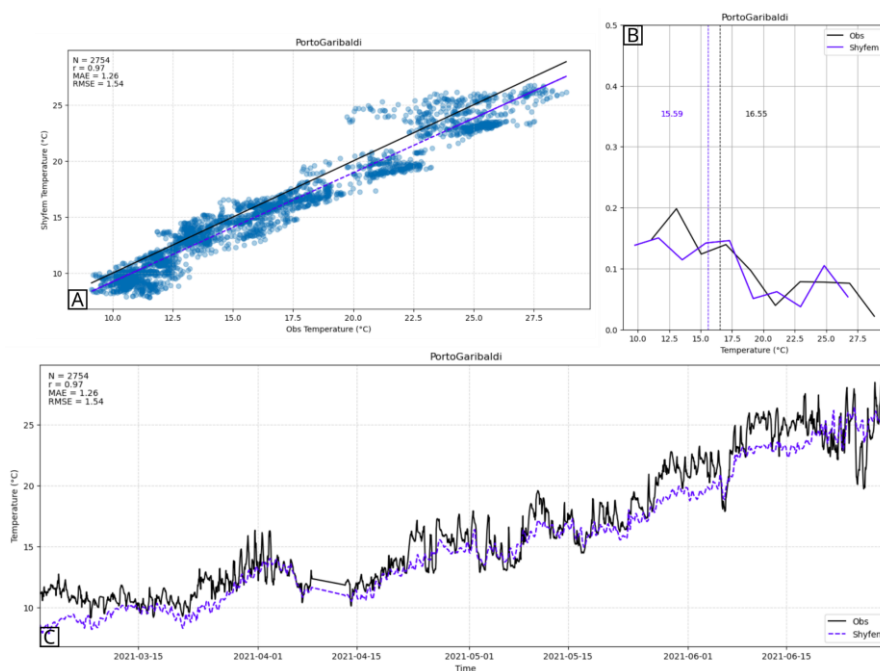


Figure 7: all subplots refer to temperature measurements at the Porto Garibaldi integrated station and the Shyfm modeled results at the closest possible location. A) scatter plot for measured and simulated temperature where the black line refers to a reference, perfect fit while the regression line in blue relates the observed data with the modeled results. B) probability distribution function for the observed data (black) and the model results (blue). C) time series of the observed data (black solid line) plotted together with the model results (blue dashed line).

For another station located inside Sacca di Goro (Venus - Figure 1C), out of the eight calibration simulations performed, the best results obtained for salinity refer to the simulation georg51 which reached a Pearson correlation value of 0.58 (together with other three simulations - LargePond, georg50_arpae, Chezy), with an MAE of 3.90PSU and a RMSE of 4.80PSU (Table 7). The time series, scatterplot, and the PDF associated with the simulation georg51 and the observed values are shown in Figure 8.

In what refers to temperature at the Venus station, the simulation georg52 outperformed the others reaching a Pearson correlation value of 0.98 (together with all other simulations), with an MAE of 1.33°C and an RMSE of 1.64°C (Table 8). The time series, scatterplot, and the PDF associated with the simulation georg51 and the observed values are shown in Figure 9.

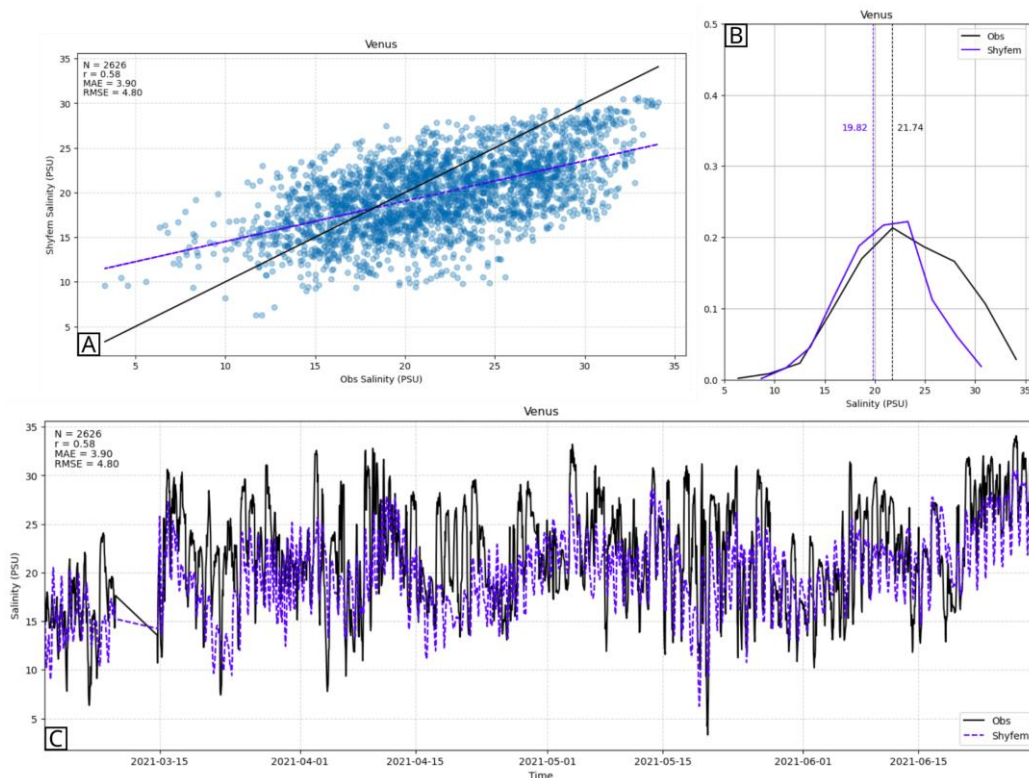


Figure 8: all subplots refer to salinity measurements at the Venus station and the Shyferm modeled results at the closest possible location. A) scatter plot for measured and simulated salinity where the black line refers to a reference, perfect fit while the regression line in blue relates the observed data with the modeled results. B) probability distribution function for the observed data (black) and the model results (blue). C) time series of the observed data (black solid line) plotted together with the model results (blue dashed line).

Table 7: statistics for salinity at the Venus measuring station for each of the calibration simulations (SIM) performed. The sampling size is shown below the name of the variable being analyzed. In bold are highlighted the values of the best performance for that specific variable for that specific station.

Venus	SALINITY (n = 2626)							
SIM	georg51	georg52	LargePond	zLBC	zLBC2	SmithBanke	georg50_arpae	Cezy
Pearson	0.58	0.57	0.58	0.57	0.57	0.57	0.58	0.58
MAE	3.90	4.41	4.06	4.17	3.94	4.16	4.38	4.28
RMSE	4.80	5.43	5.03	5.15	4.87	5.12	5.37	5.27

Table 8: statistics for temperature at the Venus measuring station for each of the calibration simulations (SIM) performed. The sampling size is shown below the name of the variable being analyzed. In bold are highlighted the values of the best performance for that specific variable for that specific station.

Venus	TEMPERATURE (n = 2695)							
SIM	georg51	georg52	LargePond	zLBC	zLBC2	SmithBanke	georg50_arpae	Cezy
Pearson	0.98	0.98	0.98	0.98	0.98	0.98	0.98	0.98
MAE	1.36	1.33	1.36	1.43	1.45	1.33	1.35	1.36
RMSE	1.67	1.64	1.68	1.76	1.77	1.65	1.66	1.68

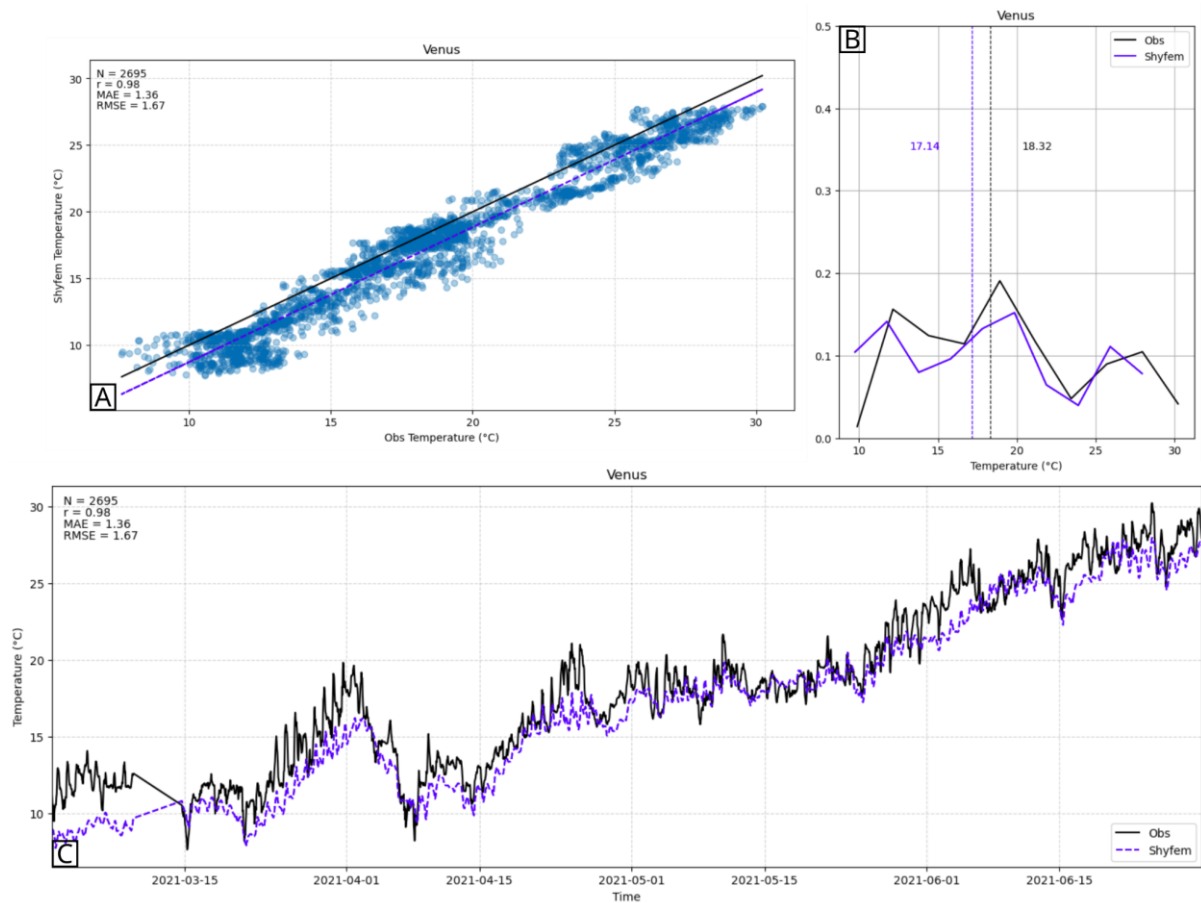


Figure 9: all subplots refer to temperature measurements at the Venus station and the Shyfer modeled results at the closest possible location. A) scatter plot for measured and simulated temperature where the black line refers to a reference, perfect fit while the regression line in blue relates the observed data with the modeled results. B) probability distribution function for the observed data (black) and the model results (blue). C) time series of the observed data

After analyzing the results of the calibration simulations, the parameter set associated with the best performance was chosen to be used in the validation as well as in other tests that were conducted and subsequently in the operational forecasting system. In order to choose the so-called best simulation, an analysis of the results was performed and the simulation with the highest number of statistical values that outperformed the other simulations chosen. Follow in Table 9 the final parameter set and in Table 10 a brief explanation of the values that have been used. In-depth information about the parameters and their meaning can be found in Shyfer's user manual (<https://github.com/SHYFEM-model/shyfer>).

Table 9: final parameter set chosen after the calibration simulations were performed and their results evaluated.

Variable	Value	Variable	Value	Variable	Value	Variable	Value
ilin	0	icor	1	itvd	0	conref	0
itlin	0	isphe	1	itvdv	0	chpar	0.1
iclin	0	ireib	6	idhtyp	2	iheat	6
itsplt	2	czdef	0.006	isalt	1	hdecay	2
coumax	0.90	iwtype	1	salref	30	botabs	0
idtsyn	'1h'	itdrag	4	shpar	0.2	ilytyp	3
idtmin	1.0	dragco	0.0025	itemp	1	hlvmin	0.5
ampar	0.60	ibarcl	1	temref	10	hmin	1
azpar	0.60	iturb	1	thpar	0.2	ihtype	3
		ievap	1	iconz	0	nomp	10

Table 10: brief description of the parameters used in the implemented model

Parameter	Brief Description	Value used
ilin	If value equals to zero, advective terms are considered	0
itlin	If value equals to zero, the usual finite element discretization is used over a single element	0
iclin	If value equals to zero, the depth term in the continuity equation is considered	0
itsplt	The biggest timestep is considered in the temporal discretization	2
coumax	Courant number	0.9
idtsyn	Interval in which a timestamp will be recorded	1h
idtmin	The smallest time step possible (s)	1.0
ampar	Weighting of the new time level of the pressure term in the momentum equations	0.6

azpar	Weighting of the new time level of the transport terms in the continuity equation	0.6
icor	If value equals to zero, Coriolis is included	1
isphe	If value equals to one, spherical coordinates are used	1
ireib	Check manual for the bottom friction calculation associated with the value used	6
czdef	Friction parameter value used in the equation denoted in the <i>ireib</i> variable	0.006
iwtype	If value equals one, the wind components are given as atmospheric forcing	1
itdrag	Formula used to compute the wind drag coefficient. If value equals four, the wind drag varies in function of the heat flux	4
dragco	Drag coefficient used in the wind drag formulation (<i>itdrag</i>)	0.0025
ibarcl	If value equals one, a full baroclinic model is considered	1
iturb	If value equals one, the GOTM turbulence closure model is used	1
ievap	If value equals one, it computes the evaporation mass flux	1
itvd	If value equals zero, an upwind scheme is used for the horizontal advection used for the transport and diffusion equation	0
itvdv	If value equals zero, an upwind scheme is used for the vertical advection used for the transport and diffusion equation	0
idhtyp	Gives the type of diffusion used in the calculations. If the value equals two, Smagorinsky is used	2
isalt	If value equals one, the model computes the transport and diffusion of salinity	1
salref	Initial salinity of the water in PSU	30
shpar	Horizontal diffusion parameter for salinity	0.2
itemp	If value equals one, the model computes the transport and diffusion of temperature	1
temref	Initial temperature of the water in centigrade	10
thpar	Horizontal diffusion parameter for temperature	0.2
iconz	If value equals zero, no concentration is calculated for a given tracer (e.g. microbiological simulations)	0
conref	If value equals zero, no reference tracer is considered (e.g. microbiological simulation)	0
chpar	Horizontal diffusion parameter for the tracer (e.g. microbiological simulation)	0.1
iheat	Type of heat flux algorithm. If the value equals six, it uses the COARE3.0 module	6
hdecay	Depth of e-folding decay of radiation (m)	2

botabs	Heat absorption at bottom [fraction]. If the value equals zero, everything is absorbed in the last layer	0
ilytyp	Treatment of the last (bottom) layer. If the value equals three, the model adds the layer thickness to the layer above if it is smaller than <i>hlvmin</i>	3
hlvmin	Minimum layer thickness for the last (bottom) layer. a value of 0.5 indicates that the last layer should be at least half of the full layer	0.5
hmin	Minimum water depth (most shallow) for the whole basin	1
ihype	How the water vapor content is specified. If the value equals three, the dew point temperature is used	3
nomp	Number of OMP threads to use	10

2.3 MODEL VALIDATION

Validation was performed using the parameter set that achieved best results during the calibration phase (Table 9). Below, validation phase scores for the analyzed variables are shown. It is important to emphasize that the analyses performed here do not consider the first two months of the simulation as they are used as spin-up time for the system to reach a stable condition.

The validation was performed trying to cover the same variables for the same stations as during the calibration phase. However, some of the stations had inconsistent data or the datasets were too short. Hence, in Figures 10, 12, and 15 the validation results for salinity at the stations of Gorino, Porto Garibaldi and Venus are shown, respectively. In Figure 13, the total water level validation results are presented while in Figures 11, 14, and 16 the validation results for temperature in the stations of Mitili, Porto Garibaldi and Venus are plotted, respectively.

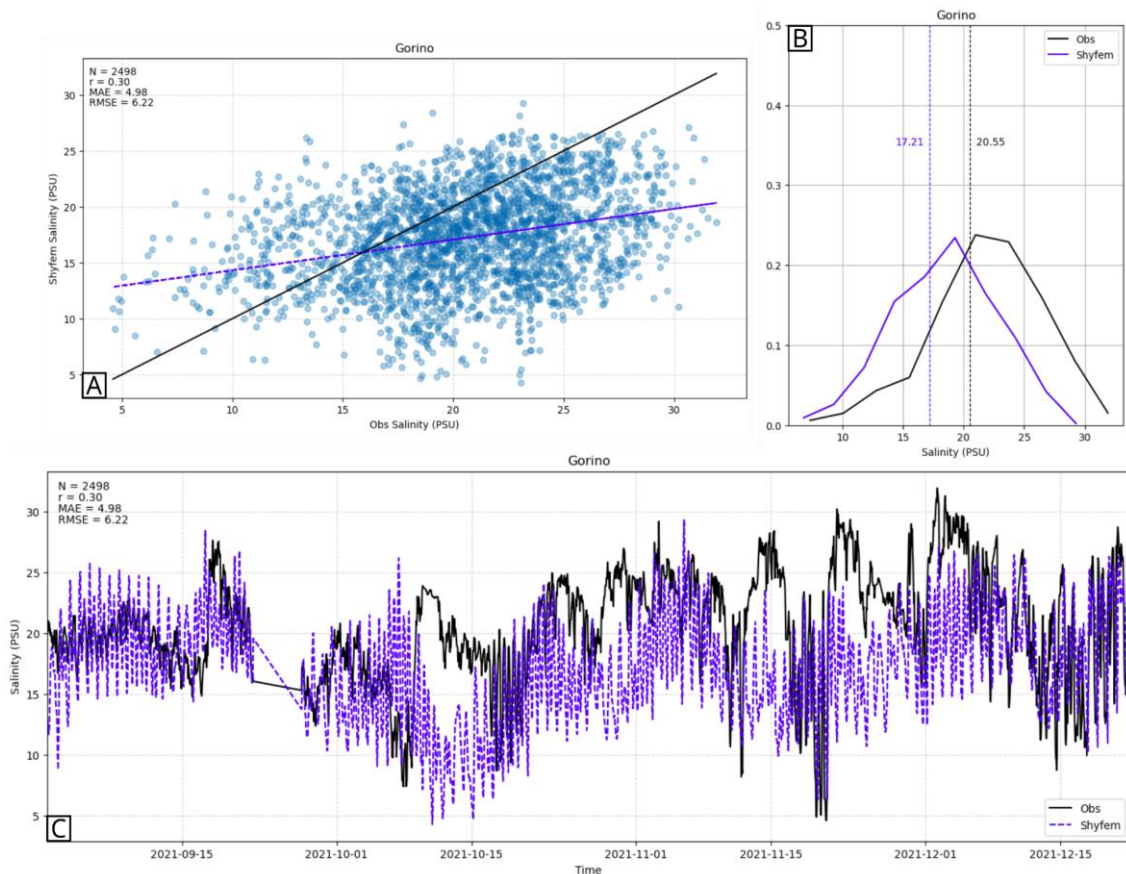


Figure 10: all subplots refer to salinity measurements at the Gorino station and the Shyferm modeled results at the closest possible location. A) scatter plot for measured and simulated salinity where the black line

refers to a reference, perfect fit while the regression line in blue relates the observed data with the modeled results. B) probability distribution function for the observed data (black) and the model results (blue). C) time series of the observed data (black solid line) plotted together with the model results (blue dashed line).

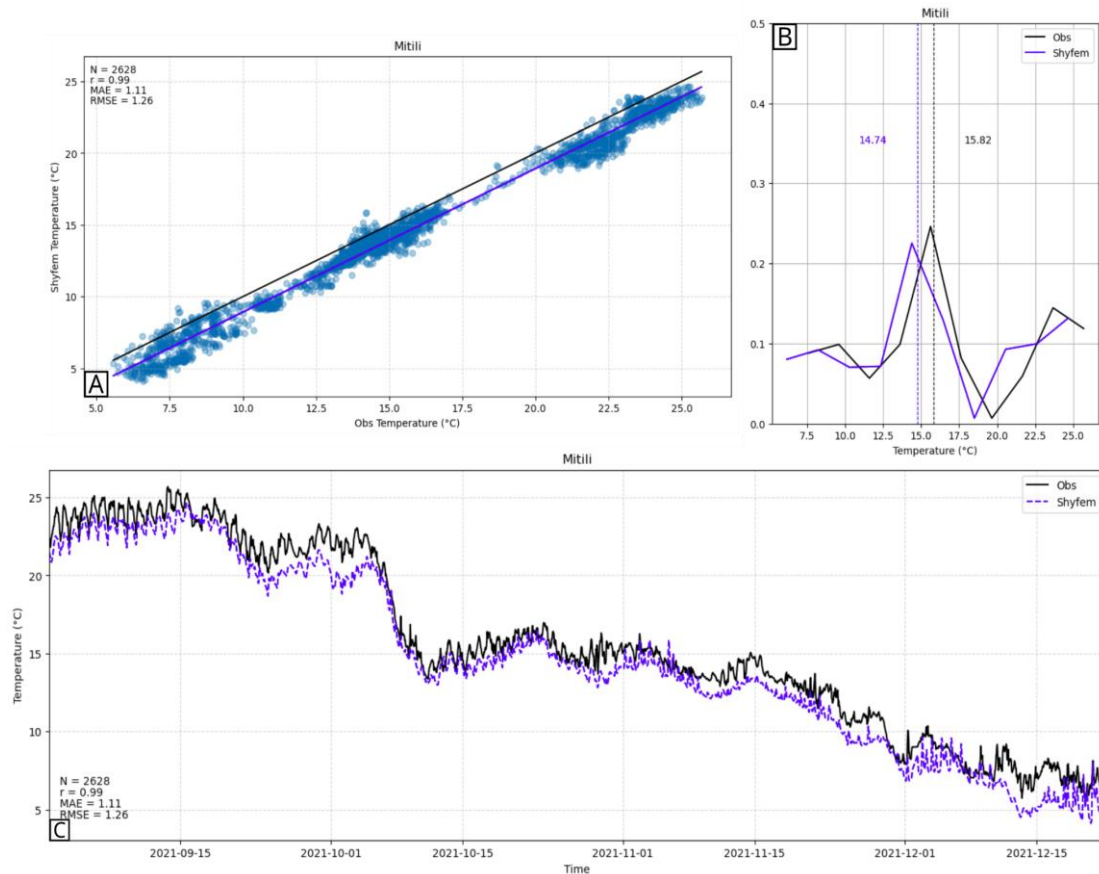


Figure 11: all subplots refer to temperature measurements at the Mitili station and the Shyferm modeled results at the closest possible location. A) scatter plot for measured and simulated temperature where the black line refers to a reference, perfect fit while the regression line in blue relates the observed data with the modeled results. B) probability distribution function for the observed data (black) and the model results (blue). C) time series of the observed data (black solid line) plotted together with the model results (blue dashed line).

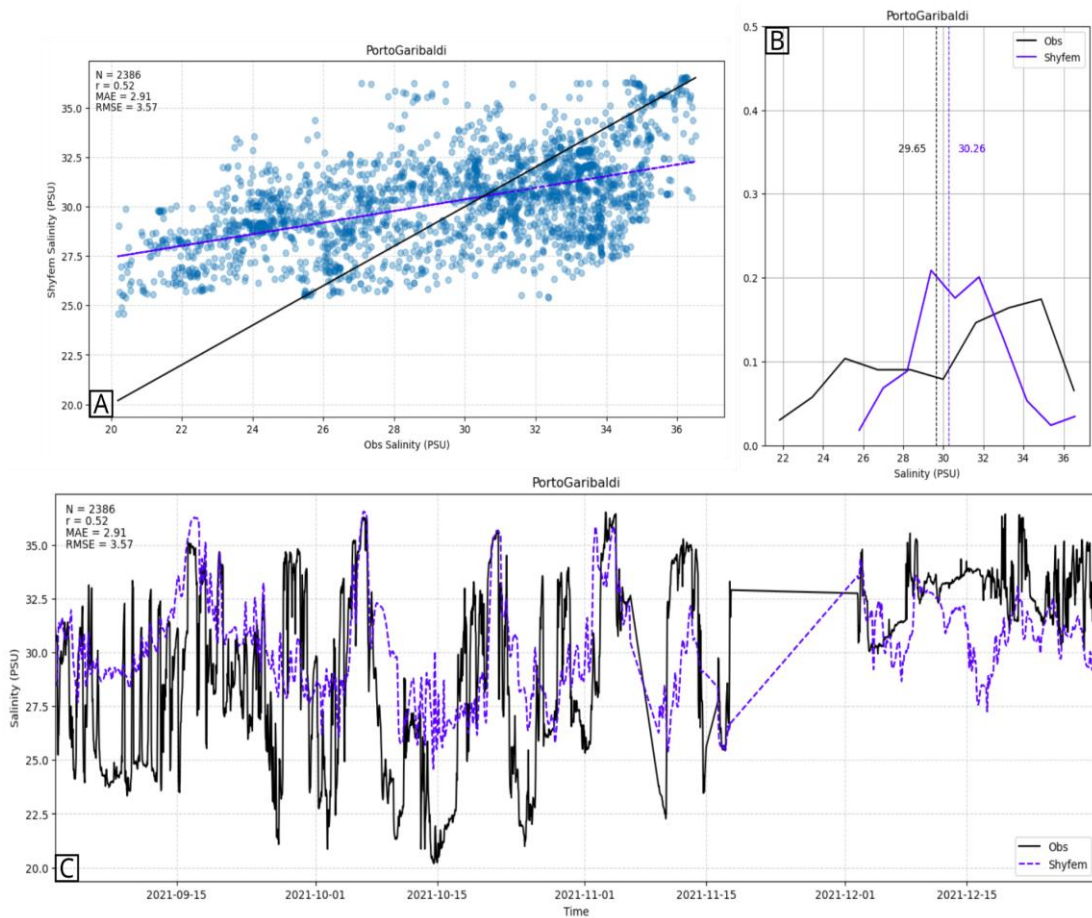


Figure 12: all subplots refer to salinity measurements at the Porto Garibaldi station and the Shyferm modeled results at the closest possible location. A) scatter plot for measured and simulated salinity where the black line refers to a reference, perfect fit while the regression line in blue relates the observed data with the modeled results. B) probability distribution function for the observed data (black) and the model results (blue). C) time series of the observed data (black solid line) plotted together with the model results (blue dashed line).

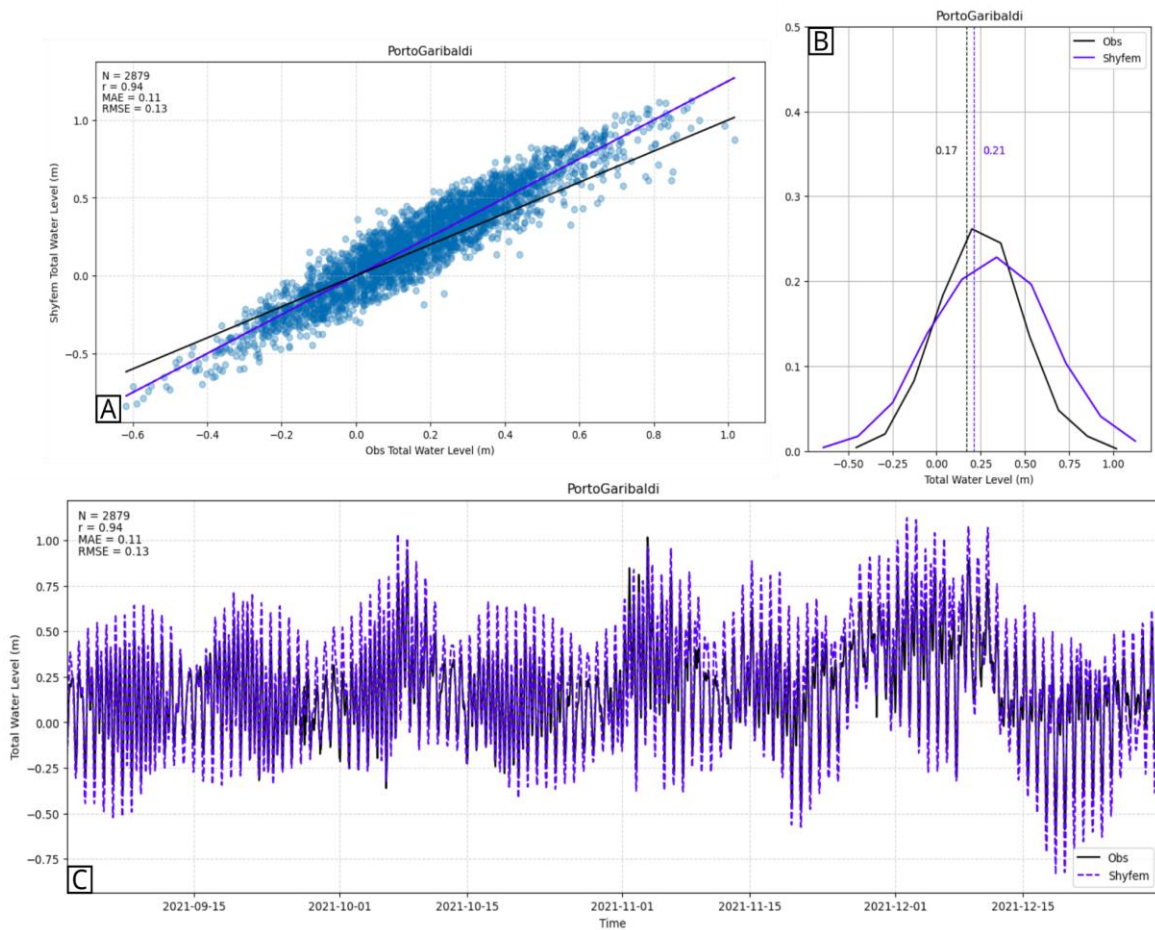


Figure 13: all subplots refer to total water level measurements at the Porto Garibaldi station and the Shyferm modeled results at the closest possible location. A) scatter plot for measured and simulated total water level where the black line refers to a reference, perfect fit while the regression line in blue relates the observed data with the modeled results. B) probability distribution function for the observed data (black) and the model results (blue). C) time series of the observed data (black solid line) plotted together with the model results (blue dashed line).

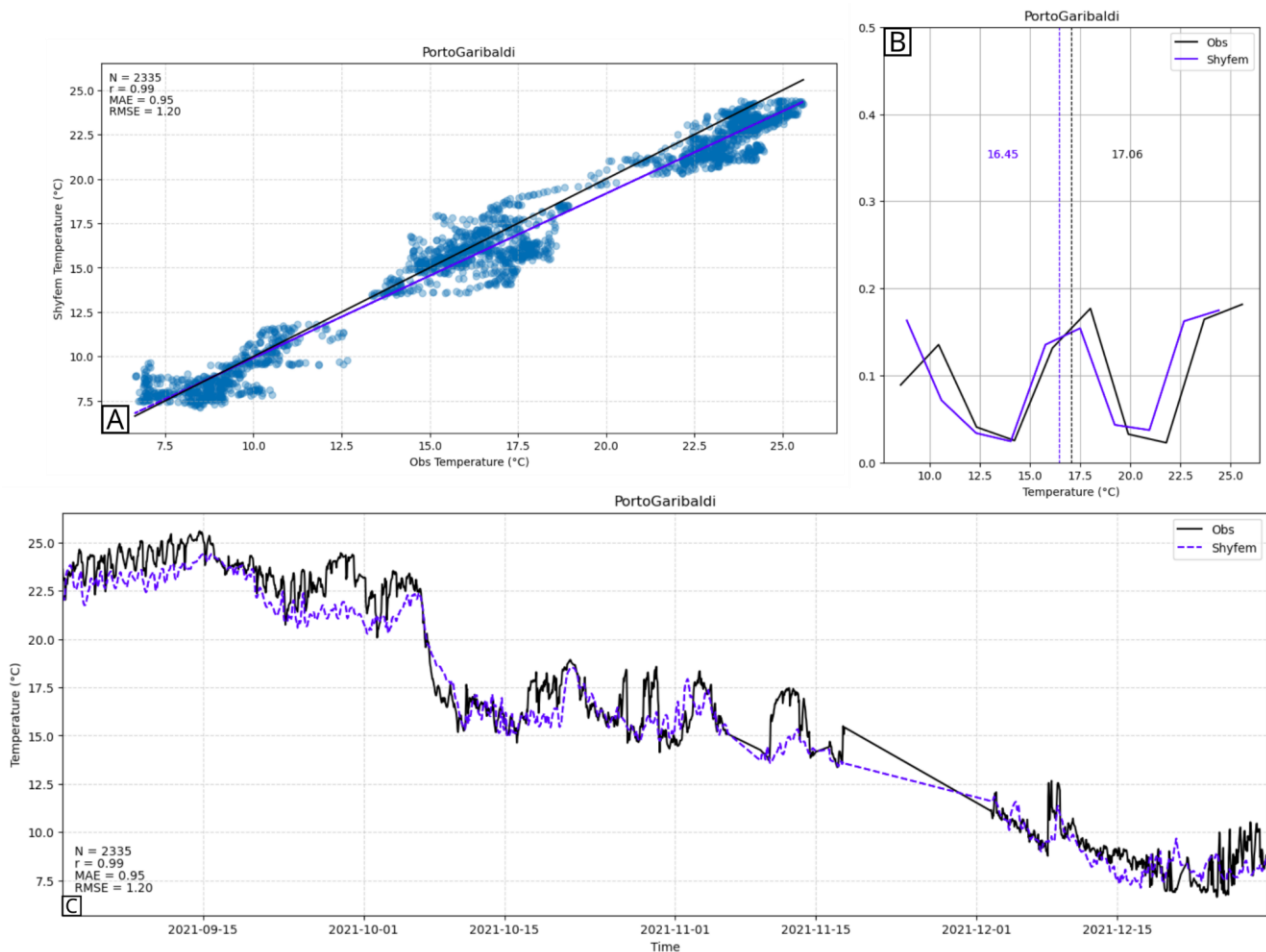


Figure 14: all subplots refer to temperature measurements at the Porto Garibaldi station and the Shyferm modeled results at the closest possible location. A) scatter plot for measured and simulated temperature where the black line refers to a reference, perfect fit while the regression line in blue relates the observed data with the modeled results. B) probability distribution function for the observed data (black) and the model results (blue). C) time series of the observed data (black solid line) plotted together with the model results (blue dashed line).

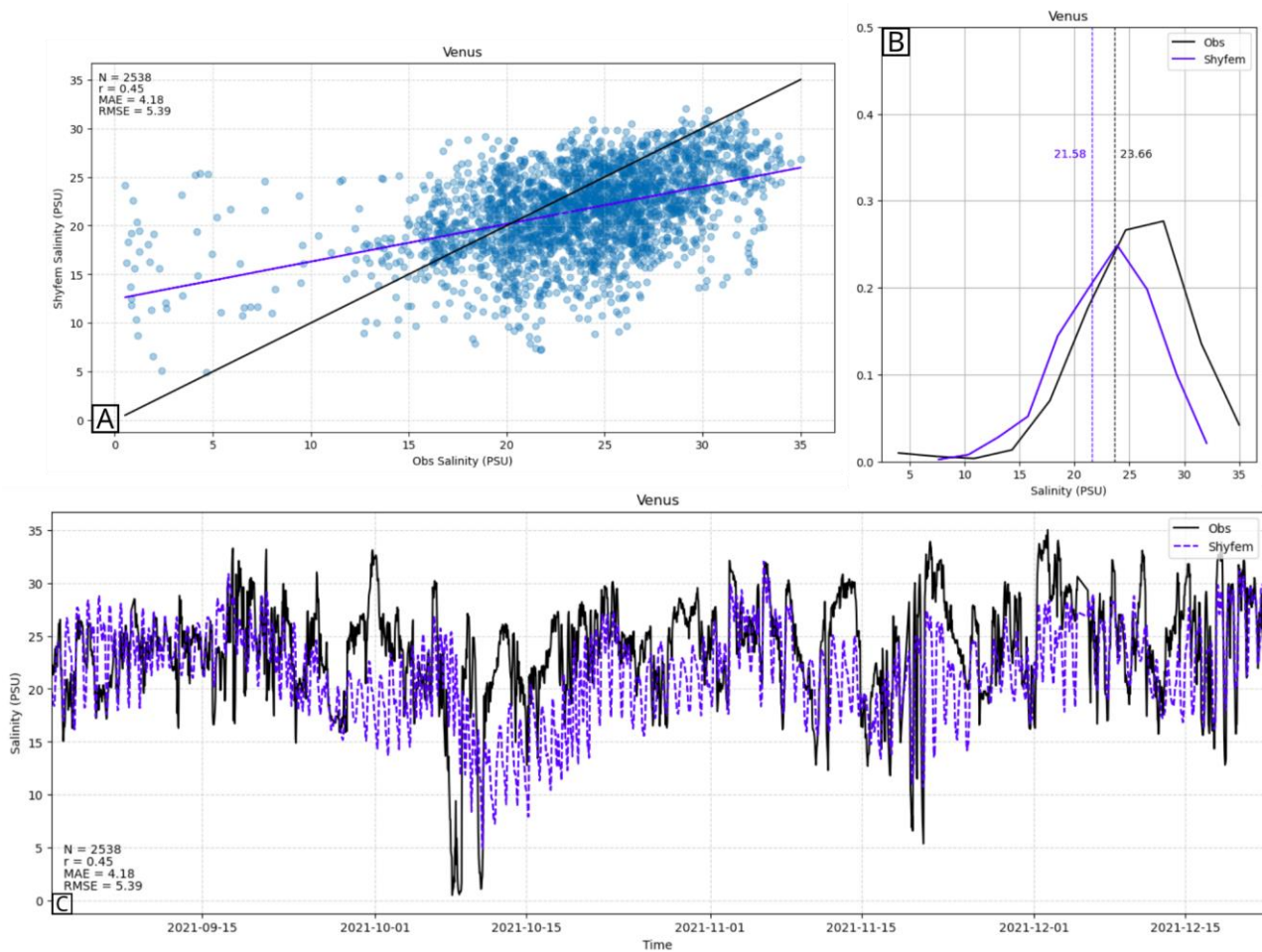


Figure 15: all subplots refer to salinity measurements at the Venus station and the Shyferm modeled results at the closest possible location. A) scatter plot for measured and simulated salinity where the black line refers to a reference, perfect fit while the regression line in blue relates the observed data with the modeled results. B) probability distribution function for the observed data (black) and the model results (blue). C) time series of the observed data (black solid line) plotted together with the model results (blue dashed line).

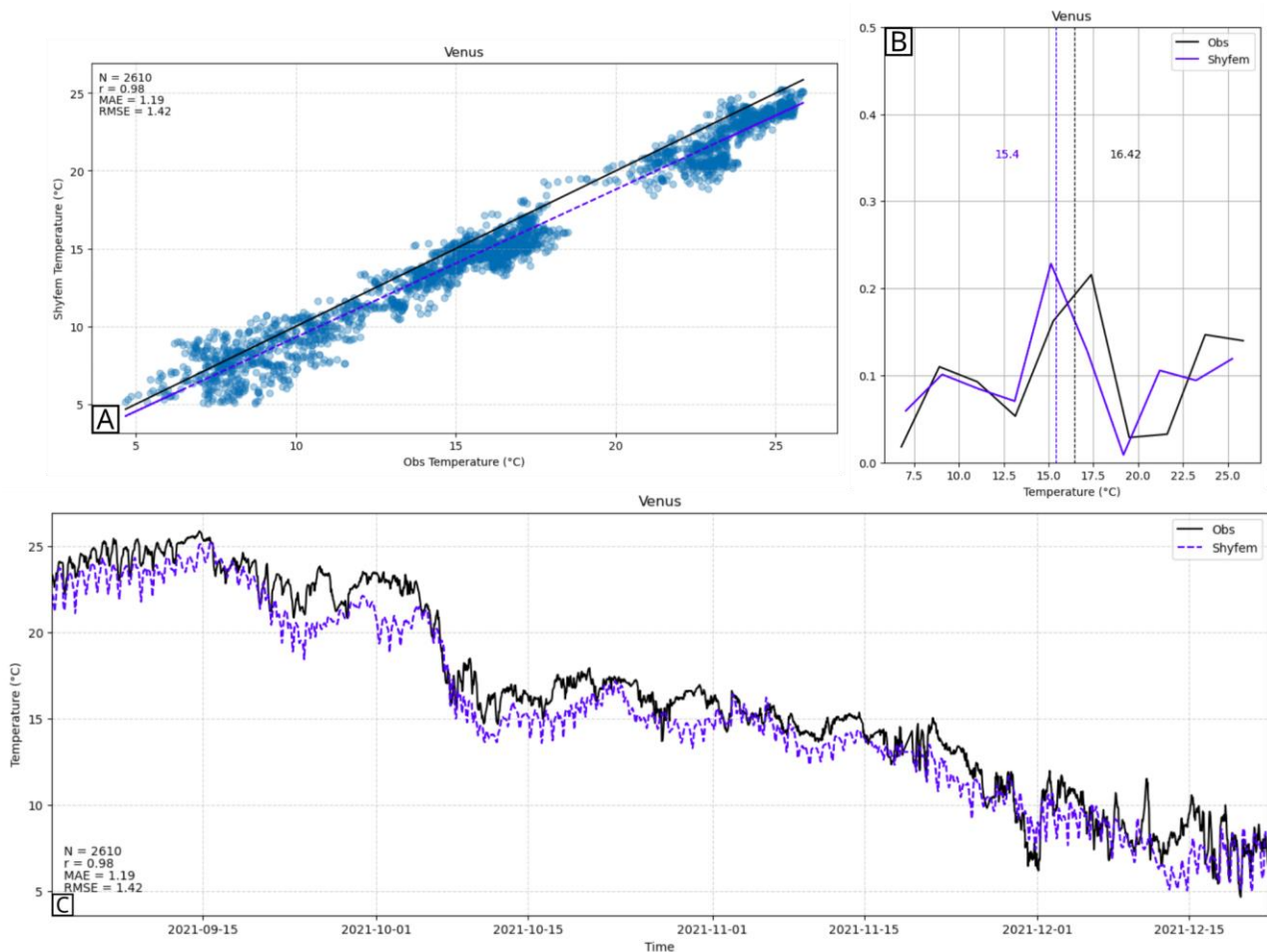


Figure 16: all subplots refer to temperature measurements at the Venus station and the Shyferm modeled results at the closest possible location. A) scatter plot for measured and simulated temperature where the black line refers to a reference, perfect fit while the regression line in blue relates the observed data with the modeled results. B) probability distribution function for the observed data (black) and the model results (blue). C) time series of the observed data (black solid line) plotted together with the model results (blue dashed line).

The performance of shyfER for the analyzed variables was considered very satisfactory. Even though the salinity and temperature present biases, they are of difficult representation in transitional environments such as the lagoons of the Po Delta system. In such environments, fast fluctuations might happen as a consequence of short-scale processes (e.g. opening and closing of water pumps) which are difficult, if not impossible, to predict. However, in general terms, the daily variations associated with the tidal cycles (semi-diurnal behavior) are well-represented, even more for the second half of 2021. For the stations located slightly offshore, the system is very susceptible to the

boundary conditions coming from the parent model(s). In shyfER specific case, temperature and salinity come from a ROMS implementation for the whole Adriatic Sea which might have its own biases (yet to be investigated).

2.4 OPERATIONAL IMPLEMENTATION AND PRODUCTS

The initial conditions for the operational system were initially set to 10°C and 30PSU for temperature and salinity, respectively. While the technical development was undergoing, the system remained that way for just over a month (from 14/02/2023 until 18/03/2023) so the computational stability was checked and further tests carried out. On 18/03/2023, when the generation of the atmospheric forcing and the boundaries was already well established with the system restarting daily from the previous day's restart file, a three-day simulation was performed interpolating AdriaC results over the shyfER computational domain. The results of the three-day simulation were then used to restart the shyfER operational system.

After about one month and a half of the operational setting being finalized, the analyses of the total water level comparing shyfER, AdriaC and observations at the Porto Garibaldi tide gauge were performed. As it is possible to see in Figure 17A, the time series of the total water level is very similar between the two models, which actually should happen considering that shyfER uses the boundary conditions from AdriaC. Differences are mostly observed with incoming perturbations (e.g. between the 26th and 30th of March) in which deviations in the models' results relative to one another can be visualized. A possible explanation for the behavior is the considerably higher resolution of shyfER (reaching up to 200m near the coast) with the coastal processes having a higher temporal-spatial resolution.

Figures 17B and 17C show the scatter plots with the measured values in the x-axis and shyfER and AdriaC results on the y-axis, respectively. AdriaC has a much larger sample size as its outputs are given every 20 minutes versus the shyfER hourly outputs. In general, the behavior is quite similar with an underestimation of the lows and an overestimation of the highs, indicating a larger astronomical tide amplitude representation by both models relative to the observations. In those results it is possible to see that shyfER performs slightly better than AdriaC in what refers to the MAE while AdriaC has a slightly better correlation value.

Among the products being developed (yet to be fully implemented), salinity, temperature, total water level and current maps showing four different domain locations are to be produced on a daily basis to provide important information for decision-makers. In Figure 18 an example of model

outputs for the Po Delta area is shown. In those maps, the user can observe the vertically averaged values for each variable (besides the total water level which is two-dimensional). In this way, it is possible to have a general idea of the environment’s behavior and the possible outcomes following the +72h forecasts.

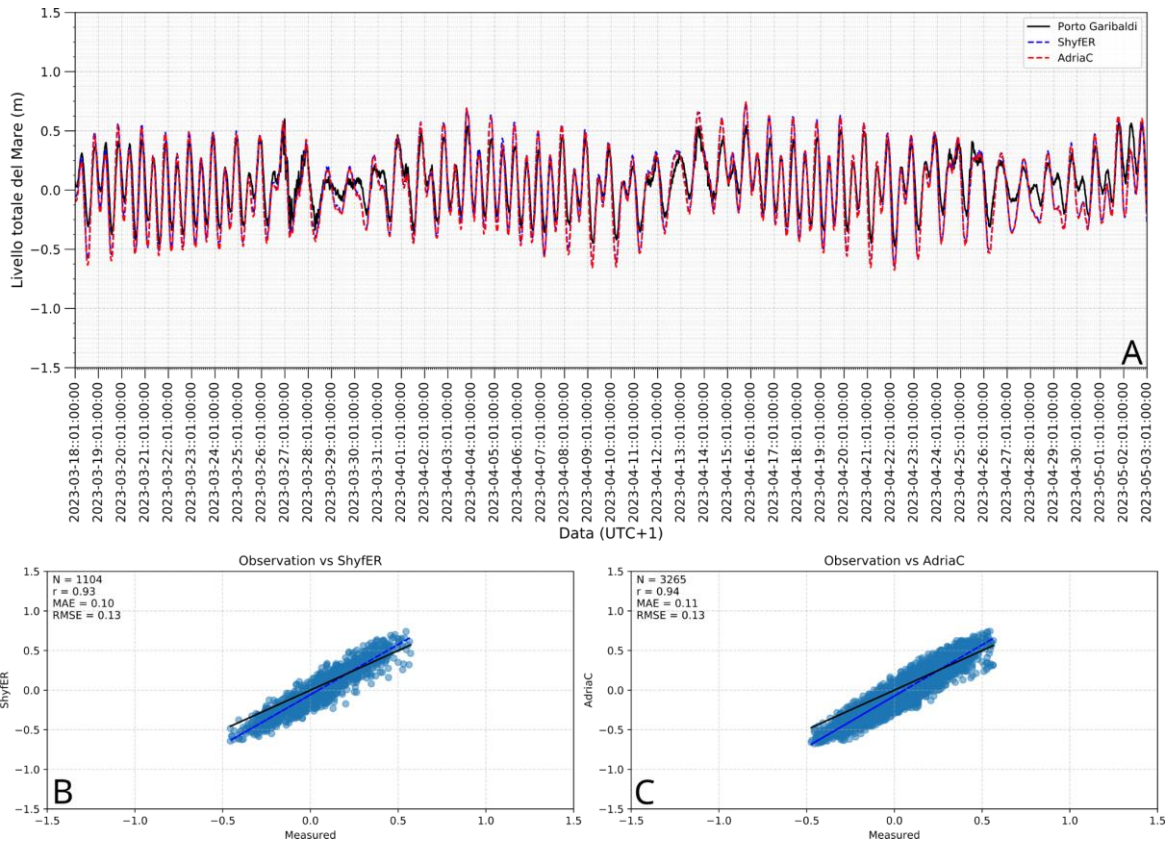


Figure 17: A) time series from 18/03/2023 until 01/05/2023 of tide gauge (black solid line), shyFER (blue dashed line) and AdriaC (red dashed line) total water level values. B) scatter plot and statistics of shyFER results relative to the observations at the Porto Garibaldi tide gauge. C) scatter plot and statistics of AdriaC results relative to the observations at the Porto Garibaldi tide gauge.

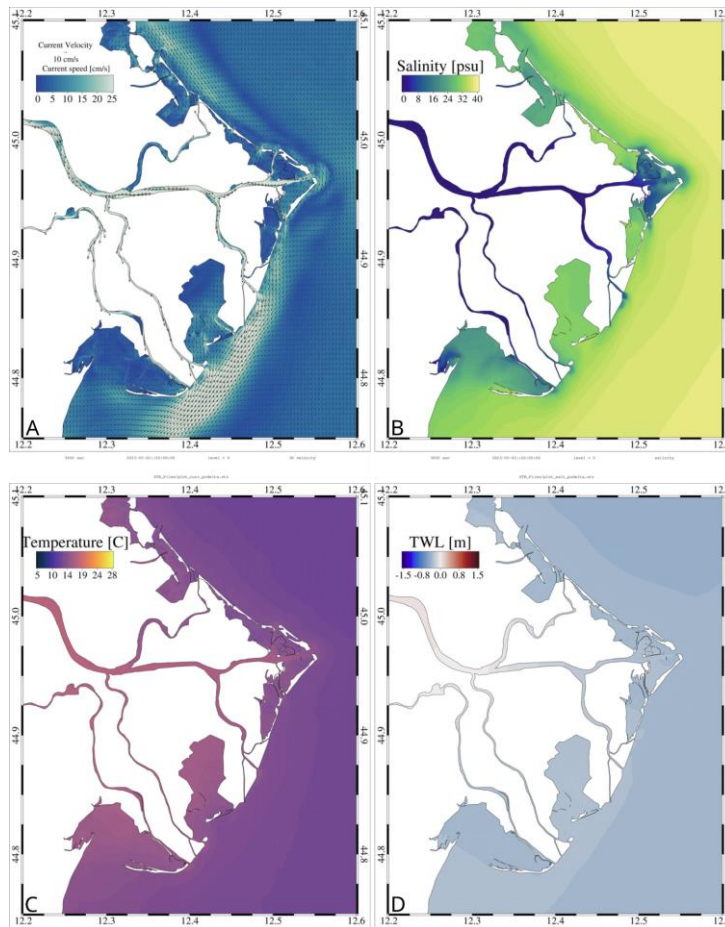


Figure 18: Zoom of the Po Delta area showing its associated lagoons and the Po River branches. All the subplots presented refer to vertically averaged values (besides the total water level - TWL) for 02/05/2023 at 2.00AM (UTC). A) Map of the distribution of currents in the Po Delta area. The colorbar presents the intensity of the currents in cm/s while the arrows indicate also their direction. B) Map of the salinity distribution in the Po Delta area. C) Map of the temperature distribution in the Po Delta area. D) Map of the TWL distribution in the Po Delta area.

If a broader scale understanding is necessary, the end user might also be interested in the maps shown in Figures 19 and 20. The former refers to the Southern Portion of the Emilia-Romagna region while the latter shows the Northern part of the domain comprehending the whole Po Delta all the way inland until Pontelagoscuro. In the larger scale maps, the user can check for larger circulation structures and, depending on the colorbar definition, see with much higher precision the variation of the variables and how they can relate to the circulation patterns.

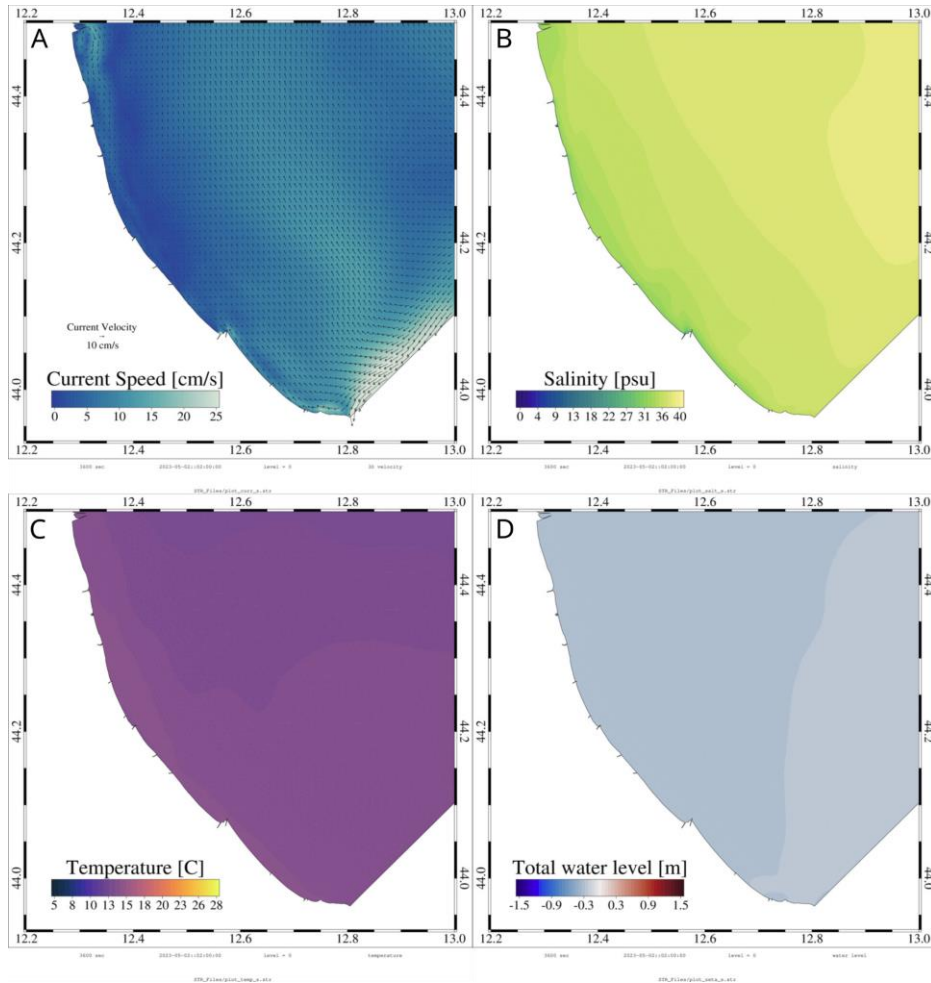


Figure 19: Zoom of the Emilia-Romagna center-South coastal area. All the subplots presented refer to vertically averaged values (besides the total water level - TWL) for 02/05/2023 at 2.00AM (UTC). A) Map of the distribution of currents in the Emilia-Romagna center-South coastal area. The colorbar presents the intensity of the currents while the arrows also indicate their direction. B) Map of the salinity distribution in the Emilia-Romagna center-South coastal area. C) Map of the temperature distribution in the Emilia-Romagna center-South coastal area. D) Map of the TWL distribution in the Emilia-Romagna center-South coastal area.

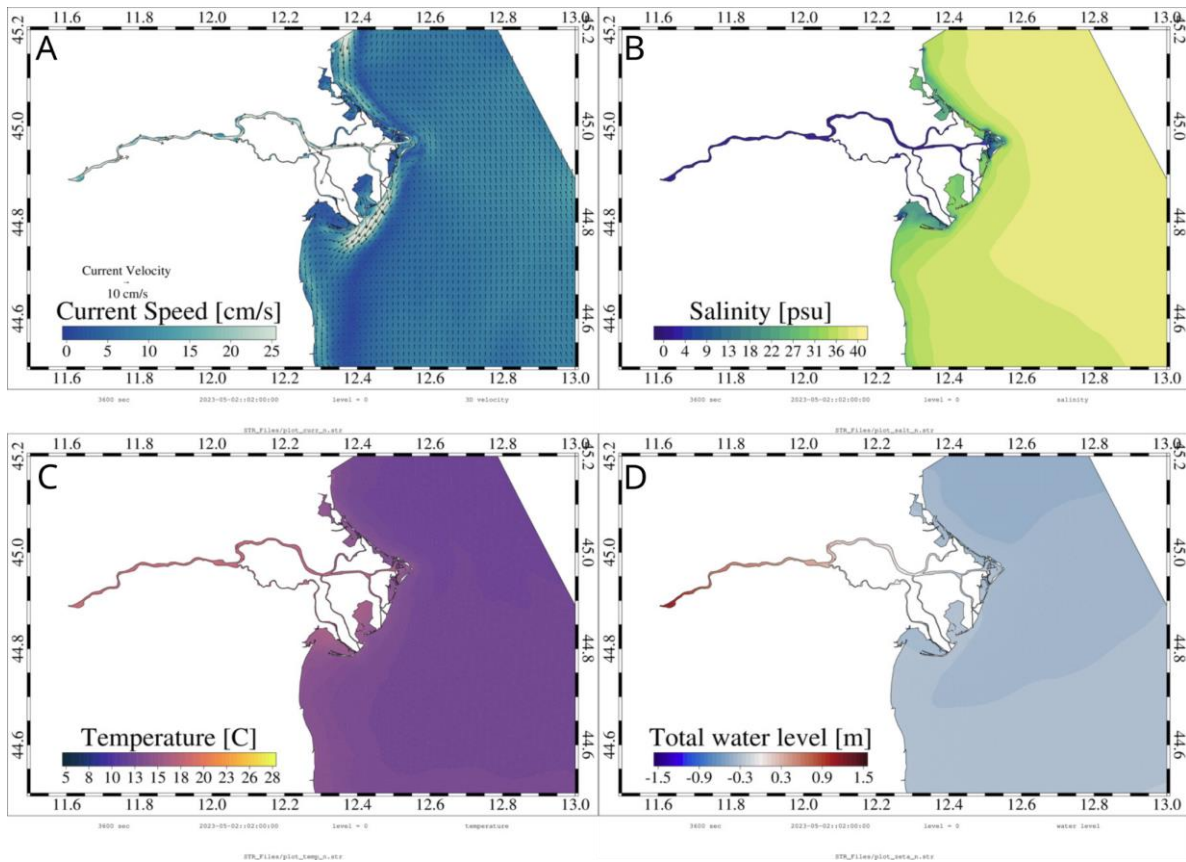


Figure 20: Zoom of the center-North Emilia-Romagna coast and the Po Delta. All the subplots presented refer to vertically averaged values (besides the total water level - TWL) for 02/05/2023 at 2.00AM (UTC). A) Map of the distribution of currents in the center-North Emilia-Romagna coast and the Po Delta. The colorbar presents the intensity of the currents while the arrows also indicate their direction. B) Map of the salinity distribution in the center-North Emilia-Romagna coast and the Po Delta. C) Map of the temperature distribution in the center-North Emilia-Romagna coast and the Po Delta. D) Map of the TWL distribution in the center-North Emilia-Romagna coast and the Po Delta.

CONCLUSIONS

It is important to emphasize that shyfER is able to represent high-frequency changing conditions following vertical water excursions as well as the seasonal temperature and salinity variations. In this case, a new system providing high-resolution forecasts and being able to solve such a detailed and complex system might provide new tools for decision-making at a regional level.

Depending on users' demands it is also possible to create maps and time series for specific locations and choose different vertical levels. For instance, if someone is interested in the vertical salinity variation in one of the Po discharge mouths, it is possible to create transects to analyze the vertical and horizontal behavior of the interface salt/freshwater. However, specific calibration might be necessary for achieving high-quality results as salt wedge modelling and forecasting can be of very difficult representation.

Yet to be done is the evaluation of the model performance in terms of salinity and temperature for stations both in the transition areas (e.g. inside the Lagoon systems) as well as in the Adriatic coastal waters. Assessing the operational system performance also in terms of salinity and temperature can provide a better understanding of possible biases that might be associated either with the oceanographic or hydrologic boundary conditions. However, some of the salinity and temperature stations that were used in the calibration and validation steps were discontinued or upgraded. Nonetheless, in the context of Interreg Italy-Croatia Projects, Arpae managed to acquire and install new multiparametric stations, a new wave buoy and new tide gauge systems which will be further used to analyze shyfER's performance.

Another potential application of shyfER outputs involves a further downscaling of its results toward even higher-resolution domains. For instance, the usage of two-dimensional flooding models (e.g. LISFLOOD, SWASH) can provide bidimensional maps that allow the user to understand the extent of flooding conditions in areas in which digital terrain and/or digital elevation models are available (DTMs and DTEs).

In order to improve shyfER's capacity, adding a data assimilation scheme to its structure might provide even closer to reality initial conditions. Such improvement might be difficult to conceptualize as data assimilation can be done point based (e.g. from a single measuring station) or from satellite imagery (which covers only the top layer of the water body - sea, lagoon, river branch - being addressed).

In order to finalize the implementation of the system, one final step is still undergoing. The model results will be sent to the multi-model system comprehending the whole Adriatic Sea providing high-resolution results that can improve the accuracy of the results at least for this particular region. This step should be finalized by the end of the STREAM project. In the meanwhile, the implementation is operationally running and provides daily forecasts/outputs.

REFERENCES

- Bellafiore, D., Umgiesser, G., 2010. Hydrodynamic coastal processes in the North Adriatic investigated with a 3D finite element model. *Ocean Dynamics* 60, 255–273. <https://doi.org/10.1007/s10236-009-0254-x>
- Chikita, K.A., Uyehara, H., Mamun, A. Al, Umgiesser, G., Iwasaka, W., Hossain, M.M., Sakata, Y., 2015. Water and heat budgets in a coastal lagoon controlled by groundwater outflow to the ocean. *Limnology* 16, 149–157. <https://doi.org/10.1007/s10201-015-0449-4>
- Cucco, A., Umgiesser, G., 2006. Modeling the Venice Lagoon residence time. *Ecological Modelling* 193, 34–51. <https://doi.org/10.1016/j.ecolmodel.2005.07.043>
- De Pascalis, F., Pérez-Ruzafa, A., Gilabert, J., Marcos, C., Umgiesser, G., 2012. Climate change response of the Mar Menor coastal lagoon (Spain) using a hydrodynamic finite element model. *Estuarine, Coastal and Shelf Science* 114, 118–129. <https://doi.org/10.1016/j.ecss.2011.12.002>
- Ferrarin, C., Roland, A., Bajo, M., Umgiesser, G., Cucco, A., Davolio, S., Buzzi, A., Malguzzi, P., Drofa, O., 2013. Tide-surge-wave modelling and forecasting in the Mediterranean Sea with focus on the Italian coast. *Ocean Modelling*. 61, 38–48. <https://doi.org/10.1016/j.ocemod.2012.10.003>
- Steppeler, J., Doms, G., Schättler, U., Bitzer, H.W., Gassmann, A., Damrath, U., Gregoric, G., 2003. Meso-gamma scale forecasts using the nonhydrostatic model LM. *Meteorology and Atmospheric Physics* 82, 75–96. <https://doi.org/10.1007/s00703-001-0592-9>
- Umgiesser, G., Canu, D.M., Cucco, A., Solidoro, C., 2004. A finite element model for the Venice Lagoon. Development, set up, calibration and validation. *Journal of Marine Systems* 51, 123–145. <https://doi.org/10.1016/j.jmarsys.2004.05.009>
- Warner, J.C., Armstrong, B., He, R. and Zambon, J.B., 2010. Development of a coupled ocean–atmosphere–wave–sediment transport (COAWST) modeling system. *Ocean modelling*, 35(3), pp.230-244.